Appl Biochem Biotechnol (2012) 168:183–197
DOI 10.1007/s12010-011-9407-8

The Effect of Ni^{2+} and Cu^{2+} on the Photocatalytic Degradation of Dyes by the Chitosan–TiO_2 Complex

Xiaolei Zhao · Gang Xiao · Xin Zhang · Haijia Su · Tianwei Tan

Received: 15 February 2011 / Accepted: 6 October 2011 /
Published online: 22 October 2011

Abstract The present research combines biosorption and photocatalysis in a functional TiO_2-immobilized chitosan adsorbent (CTA). CTA can degrade organic pollutants and adsorb metal ions simultaneously. Target pollutants were dyes of cationic (rhodamine B, Rh.B) and anionic (methyl orange, MO) nature, with Ni^{2+} and Cu^{2+} selected as heavy metals. The presence of Ni^{2+} or Cu^{2+} improved the degradation ability of CTA for MO, but inhibited the degradation of Rh.B, with Cu^{2+} exhibiting stronger effects than Ni^{2+}. There was no significant difference in CTA activity when the metal ions were pre-adsorbed or when they coexisted in the solution with the organic dyes. Protons in the reaction system affected the degradation performance in a similar way for Ni^{2+} and Cu^{2+} leading to a different effect on the degradation for MO and Rh.B. An X-ray photoelectron spectroscopy analysis of the binding energies of the metal ions on the surface in the presence of the cationic or anionic dyes explained the different behaviors. Since anionic and cationic dyes possess chromogenic groups of different charges, they adversely affect the production of OH• radicals when coexisting with Cu^{2+} or Ni^{2+}.

Keywords TiO_2 · Chitosan · Organic dyes · Metal ions · Adsorption · Photocatalytic degradation

Introduction

Wastewater of industrial, agricultural, and domestic origin contains a variety of pollutants [1]. Although the common pollutants (e.g., BOD, COD, SS) can be removed/destroyed by traditional techniques (e.g., settling, aerobic treatment), additional pollutants such as dyes, metal ions, phenols, siloxanes, and other organic and inorganic pollutants are now increasingly targeted since these are posing serious threats to human health and to the aquatic environment. Different physical and chemical methodologies like filtration,

X. Zhao · G. Xiao · X. Zhang · H. Su (✉) · T. Tan
State Key Laboratory of Chemical Resource Engineering, Beijing University of Chemical Technology, Beijing 100029, China
e-mail: suhj@mail.buct.edu.cn

advanced oxidation, ion exchange, membranes, photochemical reactions, and adsorption have been examined to control this specific persistent wastewater pollution [2–7]. Among these techniques, adsorption is an efficient, universal, albeit fairly expensive method used nowadays [8, 9]. Gupta et al. presented various adsorption findings for both the removal of some toxic textile and food dyes (e.g., carmoisine A, rhodamine B, basic fuchsin) and to manufacture low-cost, waste-based adsorbents (e.g., bottom ash, de-oiled soya, activated rice husks) to provide alternatives for activated carbon and reduce the associated operating costs [10–18]. Adsorption, however, only removes the organic pollutants (e.g., dyes), while their destruction requires chemical processes such as oxidation–reduction. Photocatalysis is one of the various advanced oxidation processes [19] and is an efficient technology for wastewater treatment.

Photocatalytic processes involving TiO_2 semiconductor particles under ultraviolet (UV) light irradiation have shown potential advantages to be used in several applications [20–26]. Moreover, scientific interests in semiconductor photocatalysis have grown significantly. Within the photocatalytic water/air purification and photocatalytic hydrogen production, the photogeneration of hole/electron pairs is essential, although the utilization of holes/electrons and the system processes are different. In the photocatalytic degradation of organic chemicals, valence band holes are the key elements that induce the decomposition of contaminants. TiO_2 has a high band gap energy of 3.2 eV and will generate electron–hole pairs when it is exposed to UV radiation below 380 nm due to photoexcitation [27]. The electron–hole pairs react readily with oxygen and water molecules from the environment to form superoxide (O_2•) and hydroxyl (OH•) radicals, which are responsible for the photocatalytic degradation of organic pollutants by TiO_2.

In the area of water and wastewater treatments, the photocatalytic applications of TiO_2 have been widely exploited in the decomposition of organic chemicals because of the strong resistance to photocorrosion, low operating temperature, low cost, and very low energy consumption [28, 29]: especially nanoparticles of TiO_2 offer a growing perspective. The nano-TiO_2 powder is however difficult to be reused since it is difficult to be separated from the water phase: the immobilization of nano-TiO_2 on an appropriate carrier (e.g., chelating resin, polyethylene terephthalate, modified silica, polytetrafluroethylene beads, and biological substances) can solve this problem. In its early development, well-crystallized TiO_2 particles immobilized on these carriers had to undergo a treatment at high temperature to achieve optimum photocatalytic performance, but the high temperature was shown to destroy the active structure of the thermally sensitive substrates [30–32]. Various attempts have since been undertaken in the development of new efficient carriers, and our research team demonstrated that chitosan is a good choice: as a biopolymer isolated from marine organisms, chitosan is a promising adsorbent to effectively remove heavy metal ions, with good adsorption characteristics for Ni^{2+}, Cu^{2+}, and other heavy metal ions [33–35]. Moreover, chitosan shows removal activities for some organic dyes [36]. Su et al. [37, 38] have developed a new surface molecular imprinting adsorbent made of chitosan to remove heavy metal ions.

In the research reported in the present paper, TiO_2 was added to the surface molecular imprinting chitosan and a double functional chitosan–TiO_2 adsorbent (CTA) was developed. Natural and waste waters invariably contain both organics and metal ions, and the photocatalytic degradation efficiency can be very different from solutions that contain organic pollutants alone. It is therefore essential to study the role metal ions play in the mechanism of the photocatalytic degradation of these organics. The metal ions (Ni^{2+} or Ag^{+}) adsorption and organic pollutants (methyl orange) degradation properties of CTA were studied in a previous work [38]. The present research studies the activity of CTA for anionic (methyl orange, MO, as an example) and cationic dyes (rhodamine B, Rh.B, as example), in the presence or absence of Cu^{2+} or Ni^{2+}.

Materials and Methods

Materials

Chitosan with 82% degree of deacetylation was extracted from shrimp shells in our laboratory. Titanium dioxide was used as the photocatalyst (Degussa P25, 80% anatase, 20% rutile, 50 m^2/g, primary particle size 25~30 nm, agglomerate size 80~100 nm). $NiSO_4 \cdot 6H_2O$ and $Cu(NO_3)_2 \cdot 3H_2O$, epichlorohydrin, acetic acid, EDTA, NaOH, MO-ethylenediamine tetraacetic acid disodium salt, and Rh.B were of analytical grade. The different ionic structure of MO vs. Rh.B is illustrated in Fig. 1, with MO being anionic and Rh.B being a cationic dye.

Preparation of Chitosan–TiO_2 Adsorbent

Firstly, 0.5 g chitosan and 0.2 g TiO_2 were dissolved in 20 mL of 2 vol% acetic acid. Then, 0.5 mL of a solution containing 5,000 mg/L Ni^{2+} was added into the above solution. The mixture was stirred continuously for 45 min, and 1 mL epichlorohydrin was added. The mixture was stirred for 5 h at 30 °C. The mixture was discharged into 0.25 M sodium hydroxide solution through a seven-gauge needle, and beads were instantaneously formed. The formed chitosan beads remained in the sodium hydroxide solution for 12 h and were washed with distilled water. The wet beads were put into a flask with 100 mL of 0.1 wt.% ethylenediamine tetraacetic acid disodium salt solution, stirred at 30 °C for 4 h, and then washed with distilled water. The chitosan beads were put into another flask with 50 mL of 0.05 mol/L NaOH solution and stirred at 30 °C for 2 h. Finally, the chitosan beads were washed with distilled water and dried at 60 °C for use.

Adsorption and Degradation Experiments

A 0.2-g adsorbent (dry) was added into a flask containing MO, or Rh.B, and also Ni^{2+} (50–240 mg/L) or Cu^{2+} (50—200 mg/L), respectively, for specific tests, in a 40-mL solution volume. The mixtures were shaken in a reciprocal shaker (70–80 rpm) at room temperature. The experiment was carried out with UV light at average intensity of 181.7 $\mu W/cm^2$ at 297 nm and 86.6 $\mu W/cm^2$ at 254 nm. The degradation (in percent) of organic compound was determined by mass balance calculation, as $[C_m - C_d]/C_m \times 100$ (%), where C_m and C_d are the initial concentration of organic compound and the concentration at irradiation time (minutes), respectively.

The loading capacity of metal ions was determined by mass balance calculation, as $Q_M = [C_M - C_e] \times V / W$, where Q_M is the loading capacity (milligram per gram), C_M is the initial

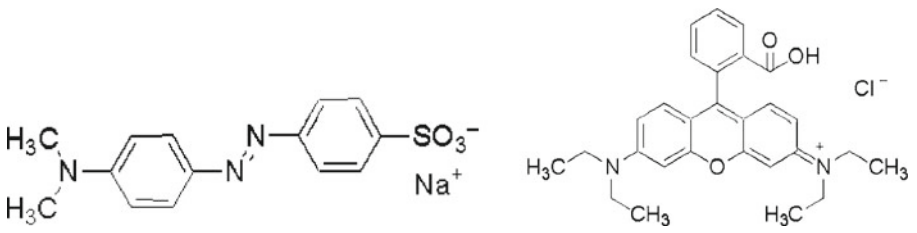

(a) (b)

Fig. 1 The structure of MO (**a**) and Rh.B (**b**)

concentration of metal ion (milligram per liter), C_e is the equilibrium concentration of metal ion (milligram per liter), V (liter) is the volume of added solution, and W (gram) is the weight of the adsorbent (dry).

Analysis

The concentrations of Ni^{2+} and Cu^{2+} were analyzed by an atomic adsorption spectrum (SpectrAA 55-B, Varian). The dye concentration was analyzed by an absorption spectrophotometer (MO at 464 nm and Rh.B at 552 nm). X-ray photoelectron spectroscopy (XPS) was used to investigate the binding energy of metal ions in the different experiments.

Results and Discussion

Effects of Coexisting Ni^{2+} on the Photodegradation of Different Organic Dyes by TiO_2

The degradation of MO and Rh.B by TiO_2 powder in the presence or absence of Ni^{2+} was examined. Table 1 shows that TiO_2 powder has a strong ability to degrade organic dyes, and the addition of Ni^{2+} into the photocatalytic system leads to the increased degradation for MO and a decrease for Rh.B by TiO_2. Without Ni^{2+}, a nearly complete degradation of MO and Rh.B was observed after UV illumination during 2 h. When Ni^{2+} was added into the reaction system, it strongly inhibited the photocatalysis efficiently of TiO_2 for Rh.B, which decreased from >99.9% to 57.8%. The degradation efficiency of TiO_2 for MO remained excellent, which can be attributed to the enhancement of the anionic MO adsorption due to electrostatic interaction with the adsorbed positively charged Ni^{2+} [39] (this interaction is opposite in the case of anionic Rh.B dye). As discussed in detail further in the text, it is suggested that the metal ions will combine electron/hole pairs with different behaviors according to the charge of the dye: MO carrying anionic charges will help the connection of metal ions and electron/hole pairs due to their complementary charges, while cationic Rh.B will have a competitive connection with metal ions. More research was therefore conducted and is discussed below.

Effects of Pre-adsorption of Metal Ions on the Degradation of MO and Rh.B by CTA

To further clarify the effect of pre-adsorbed metal ions, the degradation of anionic dye-MO and cationic dye-Rh.B was examined when metal ions (Ni^{2+} or Cu^{2+}) were pre-adsorbed. Figures 2 and 3 illustrate the degradation yield of CTA with or without metal ions being present. Pure CTA showed good degradability for both MO and Rh.B, being 52.8% and 58.3%, respectively. The pre-adsorption of metal ions has a different influence on the

Table 1 Effects of coexistence of Ni^{2+} on degradation of organic dyes by TiO_2

Different organic dyes	Concentration of Ni^{2+}(mg/L)	Degradation (%)
MO	0	>99.9
	400	>99.9
Rh.B	0	>99.9
	400	57.8

W=0.01 g, V=50 mL, t=2 h, C_m(MO)=10 mg/L, C_m(Rh.B)= 10 mg/L

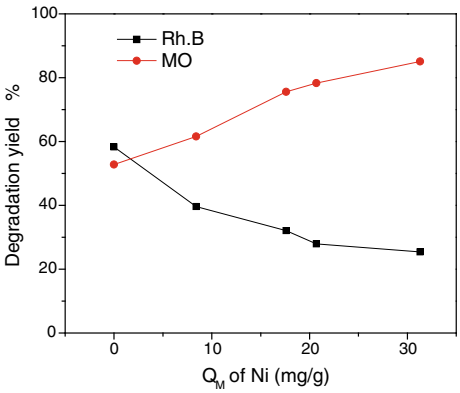

Fig. 2 Effects of pre-adsorption of Ni^{2+} on the degradation of organic dyes by CTA

degradation behavior of the CTA for MO and Rh.B, whereas the degradability of CTA for MO was enhanced after it had been loaded with metal ions (Cu^{2+} and Ni^{2+}), and the opposite occurs for Rh.B. The degradation yield of MO at 6 h increased from 52.8% to about 85.1% with the increasing Ni^{2+} load from 0 to 31.3 mg/g. When the Cu^{2+} load increased to 78.5 mg/g, the degradation yield quickly reached 86.7%. On the contrary, the degradability of the M^{2+}/chitosan/TiO_2 adsorbent for Rh.B was progressively reduced. With an increasing degree of pre-adsorption, the degradation using Ni^{2+}/chitosan/TiO_2 and Cu^{2+}/chitosan/TiO_2 adsorbent decreased to 25.4% and 11.3%, respectively.

It is well known that the photocatalysis of TiO_2 depends on the production of OH• radicals. Electron–hole pairs will be generated when TiO_2 is exposed to UV radiation, but only part of them will transfer to the surface of TiO_2 due to some electron–hole recombination inside TiO_2. Electron–hole pairs on the surface of TiO_2 interact with the reaction system and provide TiO_2 with its function as photocatalyst [40, 41]. When Ni^{2+} was pre-adsorbed on the surface of TiO_2, Ni^{2+} acts as electron acceptor to combine with the photoelectrons, thus generating more photo-induced holes. MO (Fig. 1a) with anionic chromogenic groups has a stronger ability to combine photo-induced holes than when there was no Ni^{2+} present. The opposite phenomenon was observed in the degradation of Rh.B (Fig. 1b) with cationic chromogenic groups: Rh.B will compete with Ni^{2+} to combine with photoelectrons, thereby inhibiting the separation of the election–holes and leading to a weakening of the photocatalytic abilities towards Rh.B. Similar results were observed for the degradation of MO and Rh.B when Cu^{2+} was pre-adsorbed.

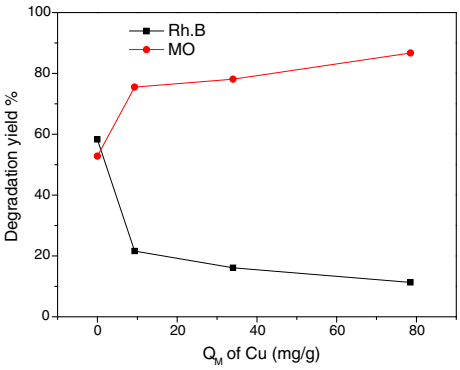

Fig. 3 Effects of pre-adsorption of Cu^{2+} on the degradation of organic dyes by CTA

Effects of the Coexistence of Metal Ions and Organic Dyes upon the Degradation by CTA

The addition of metals ions into the photocatalytic system leads to the increased degradation for MO and a decrease for Rh.B, indicating a different degradation route for different organic dyes, as explained at the end of the paper. Figure 4 shows that the degradability of MO by CTA was facilitated when the system contained MO and Ni^{2+} together. As shown in Figs. 4 and 5, the degradation yield of MO increased from 55.9% to 85.1%, and the degradation of Rh.B decreased from 53.1% to 25.2% when the Ni^{2+} concentration increasing from 0 to 240 mg/L in the solution. The effect of the coexistence of Ni^{2+} on the degradation of MO was furthermore investigated by using the Langmuir–Hinshelwood first-order kinetic model, expressed by a simple linear equation [42]: $\ln(C_m/C_d) = k_1 \cdot t$; k_1 represents the photocatalytic rate constant (per minute). Figure 6 shows the straight lines of $\ln(C_m/C_d)$ versus irradiation time whose slope corresponds to k_1 under different Ni^{2+} concentrations (from 0 to 240 mg/L). In each condition, R^2 exceeded 0.986 which indicated a good fit of the simple linear kinetic model to the experimental data. Under different cases (Ni^{2+} concentration ranging from 0 to 240 mg/L), the values of the rate constant were 0.0033, 0.0040, 0.0050, and 0.0038 min^{-1}, respectively. This indicated that the existence of metal ions promoted the degradation of anionic dyes, and the effect did not monotonously increase with the increasing ion concentration, implying that a peak value of ion concentration existed.

A similar phenomenon was observed when Cu^{2+} was present, and the degradation ratio of MO increased from 56.8% to 89.2% when the Cu^{2+} concentration increased from 0 to 200 mg/L in the solution. Contrary to MO, the degradability of Rh.B decreased by about 13.8% (Fig. 7).

These effects are the result of the interaction of metal ions and the CTA, leading to different effects when exposed to UV radiation. When Ni^{2+} (or Cu^{2+}) and MO coexisted, Ni^{2+}, as electron acceptor, combines the photoelectrons on the surface of TiO_2, so more photo-induced holes are generated. MO with anionic chromogenic groups had a stronger ability to combine photo-induced holes than when no Ni^{2+} was present. The opposite phenomenon was observed when Ni^{2+} (or Cu^{2+}) and Rh.B coexisted: Rh.B with cationic chromogenic groups will competitively combine photoelectrons with Ni^{2+} and will hence inhibit the separation of

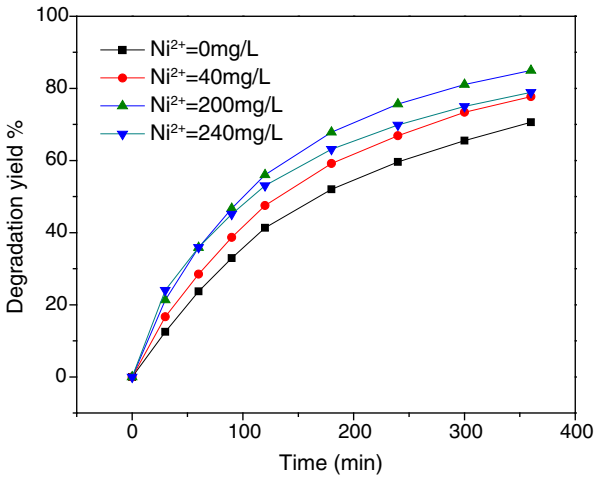

Fig. 4 Effects of the coexistence of Ni^{2+} and MO upon the degradation by CTA

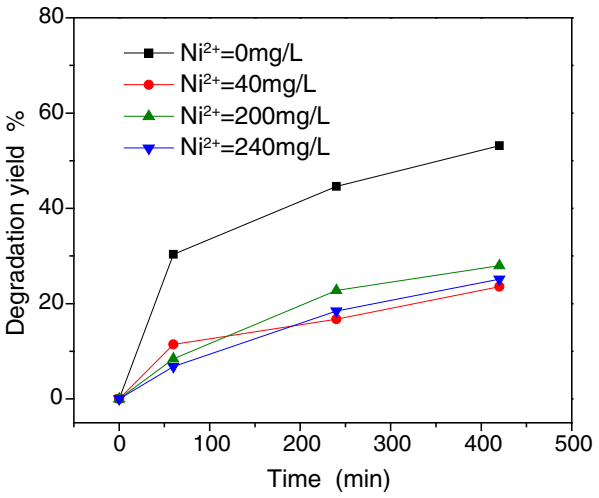

Fig. 5 Effects of the coexistence of Ni^{2+} and Rh.B upon the degradation by CTA

the election–holes and will lead to the weakening of the photocatalytic abilities for Rh.B when Ni^{2+} and Rh.B coexisted.

Table 2 summarizes the effect of the different metal forms (pre-adsorbed or coexisting) on the degradation of MO and Rh.B by CTA, showing a similar trend observed. Although the different behaviors of the Cu form are obvious, the pre-adsorbed or coexisting form has little effect in the case of Ni^{2+}. In order to clarify the common effect of metal ions, excluding the effect of their form, CTA-adsorbed Ni^{2+} was further investigated by XPS.

Effect of pH with the Coexistence of Ni^{2+} upon the Degradation by CTA and Chitosan

In the metal ion and dye coexistence system, the effects of pH include two aspects: on the one hand, in the solution with lower pH, more protons exist which act as electron acceptor

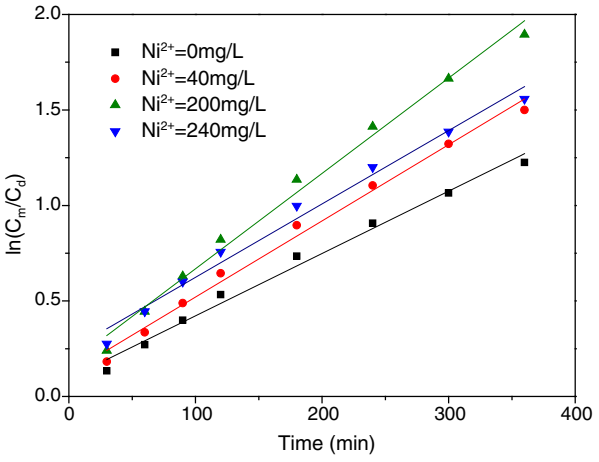

Fig. 6 Variation of $\ln(C_m/C_d)$ with irradiation time under different Ni^{2+} concentrations

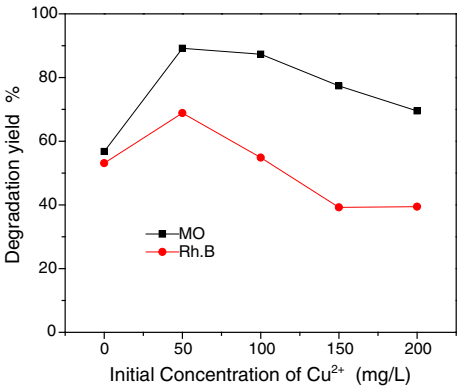

Fig. 7 Effect of Cu^{2+} concentration on degradation of MO and Rh.B (at irradiation time=6 h)

and affect the degradation for Rh.B/MO differently, just in a similar way with Ni^{2+} and Cu^{2+} (as illustrated in "Effects of the Coexistence of Metal Ions and Organic Dyes upon the Degradation by CTA"); on the other hand, a lower pH value means better dispersion and causes better interaction effects that consequently improve the elimination. Figure 8 shows the degradation of Rh.B and MO by CTA under different pH conditions (shown in solid symbols). In the case of Rh.B, more protons inhibited and better dispersion promoted the degradation by CTA, so there was a peak in the plot of degradation yield versus pH. As far as MO was concerned, more protons and better dispersion both promoted the degradation by CTA, and the degradation increased with the decreasing pH value. Figure 8 also shows the degradation of Rh.B and MO by chitosan under different pH conditions (in hollow points). A lower pH value leads to a better degradation for both Rh.B and MO when the pH value is under 5, and when it is above 5, the two plots did not change greatly which could be explained as follows: because of the absence of TiO_2, there was no electron transfer in the system of protons as electron acceptor; thus, the effects of pH on the dispersion of chitosan play as a dominant role, especially in the lower pH value.

XPS

Figure 9 and Table 3 show the XPS of Ni^{2+} at various concentrations loaded on the surface of CTA with or without dye being present (a MO, b none, c Rh.B). Table 3 shows that the binding energy of Ni^{2+} on the surface was different when the CTA degraded different organic dyes. When Ni^{2+} (C_{Ni}=200 mg/L) coexisted with MO, the binding energy was 856.42 eV, and when Ni^{2+} (C_{Ni}=200 mg/L) coexisted with Rh.B, the binding energy was 855.46 eV. A higher binding energy of Ni^{2+} would oppress the recombination rate of e−/h + pairs of TiO_2 so that it will result in stronger production of OH• radicals, which have a positive influence on the photocatalytic activity of the adsorbent for MO. But the opposite

Table 2 The effect of the metal present on the degradation by CTA

	Cu^{2+}	Pre-adsorbed (Q_M=78.5 mg/g)	Coexisting (C_M=200 mg/L)	Ni^{2+}	Pre-adsorbed (Q_M=31.3 mg/g)	Coexisting (C_M=240 mg/L)
Degradation ratio change (%)	MO	+33.9	+12.7	MO	+32.3	+29.2
	Rh.B	−47.0	−13.8	Rh.B	−32.9	−27.9

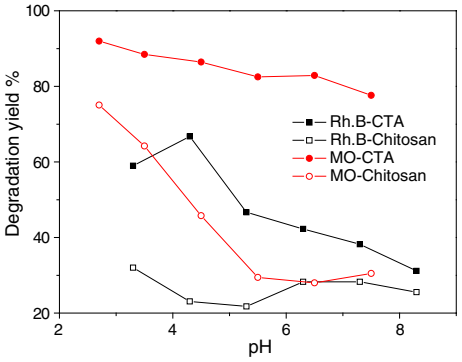

Fig. 8 Effect of pH on degradation of MO and Rh.B by CTA or chitosan. t=6 h, C_M (Ni^{2+})=200 mg/L

phenomenon was observed when Ni^{2+} and Rh.B were jointly present. The lower binding energy of Ni is unable to oppress the recombination rate of e−/h + pairs of TiO_2 efficiently, and the adsorbed and coexisting Ni^{2+} will therefore decrease the degradation of Rh.B by CTA. Clearly, the metal's ability of gaining electron affects the degradation of the CTA for organic dyes with different properties. Figure 10 and Table 3 show that there was no obvious binding energy change of Ti, meaning that the immobilization of TiO_2 onto chitosan did not alter the structure of TiO_2. Clearly, TiO_2 immobilization on chitosan offer vast perspectives in photocatalytic degradation [43].

The Photocatalysis Route of TiO_2 When Metal Ions Are Present

To further elucidate the findings of the research, the mechanism of photocatalysis offers a tentative explanation of the different behaviors noticed. The principle of photocatalysis is illustrated in Fig. 11.

It has been reported that the TiO_2 photocatalytic reactions proceed mainly by the contributions of active oxygen species, such as hydroxyl radical, OH•; superoxide radical, O_2•; and hydrogen peroxide, H_2O_2. Among them, the OH• radical is an extremely important species. Although the OH• formation mechanism has been suggested as the result of photocatalytic decomposition of water, the detailed mechanism on the TiO_2 surface is unclear so far, and a lot of efforts have been spent to elucidate the precise mechanism [44–48]. In wastewater containing both organics and metal ions, it is essential to study the role that metal ions play in the mechanism of the photocatalytic degradation of these organics. Some postulates have been put forward to explain this which include:

- Electron trapping by the metal ions leading to the prevention of electron–hole recombination or competitive combination with photoelectrons [49–51]
- A homogeneous, Fenton-type reaction mechanism induced by the presence of the dissolved transition metal ions [52, 53]
- The formation of the TiO_2–metal systems [54, 55]

Table 3 Binding energy of Ni and Ti when adsorbed with different organic dyes (a MO, b none, c Rh.B)

a	Peak BE	b	Peak BE	c	Peak BE
Ni2p3	856.42	Ni2p3	855.64	Ni2p3	855.46
Ti2p3	458.95	Ti2p3	459.08	Ti2p3	459.03

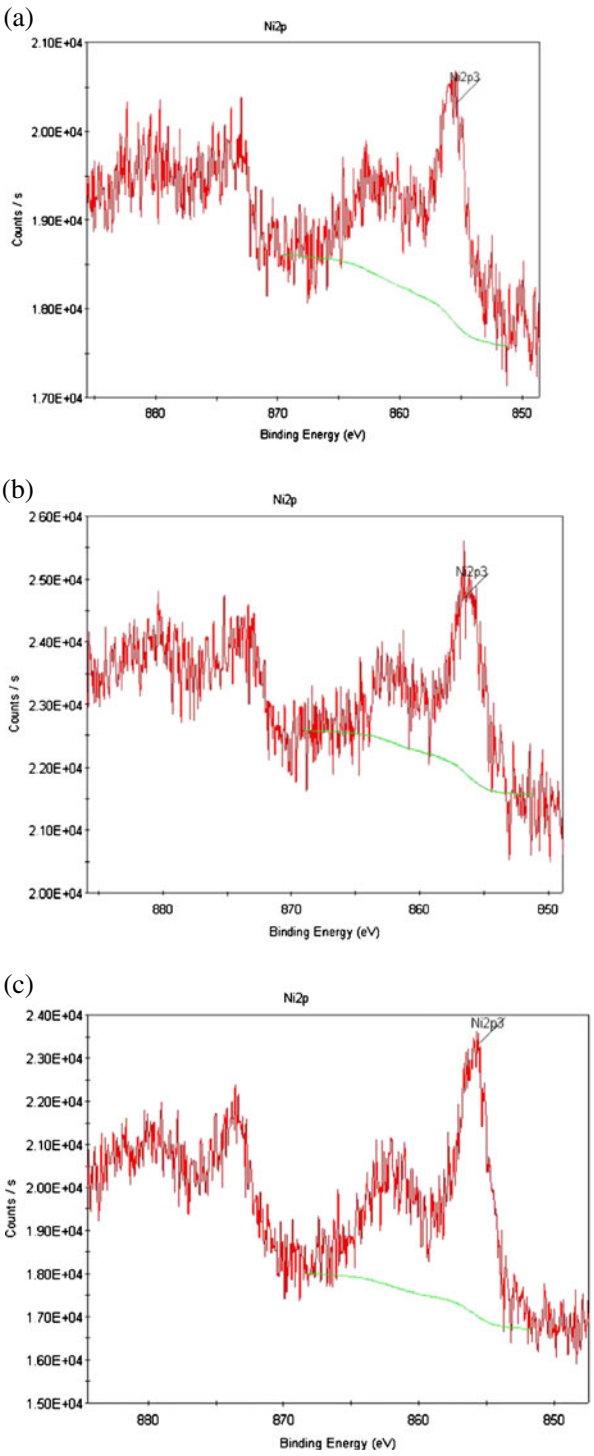

Fig. 9 XPS spectra of Ni *2p* when adsorbed with different organic dyes (**a** MO, **b** none, **c** Rh.B). C_{Ni}=200 mg/L, C_{dyes}=10 mg/L

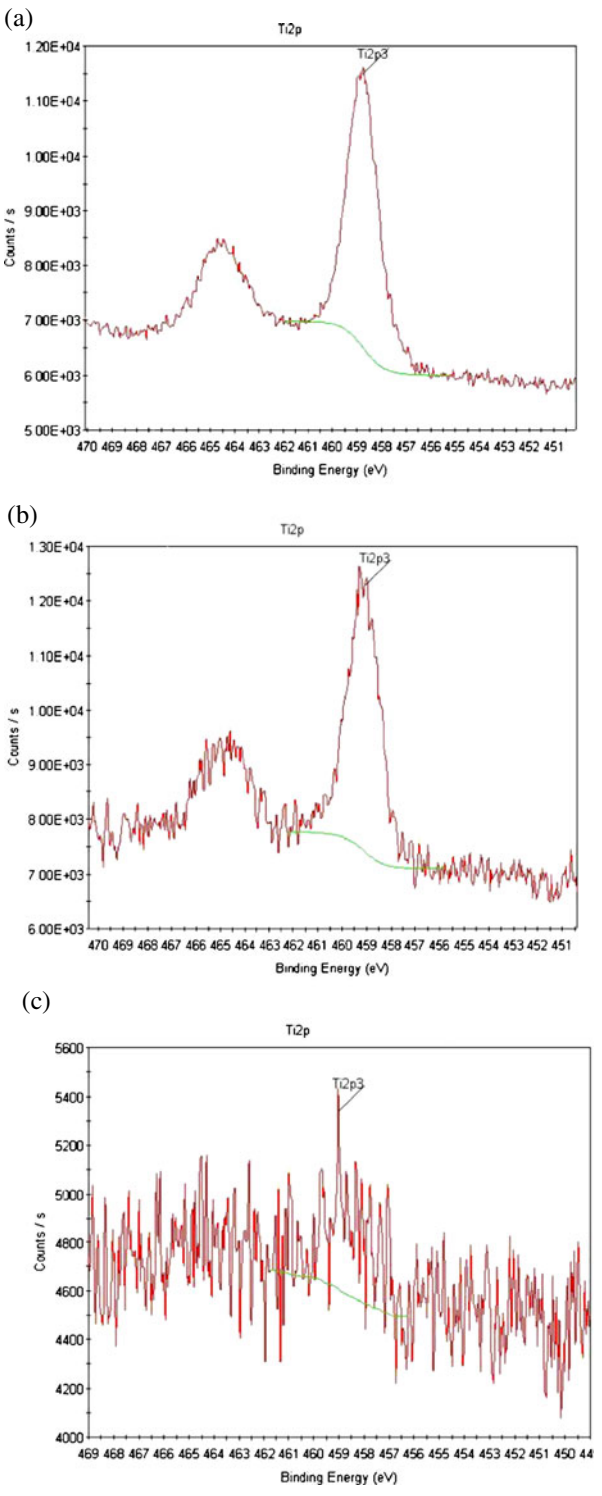

Fig. 10 XPS spectra of Ti *2p* when adsorbed with different organic dyes (**a** MO, **b** none, **c** Rh.B). C_{Ni}=200 mg/L, C_{dyes}=10 mg/L

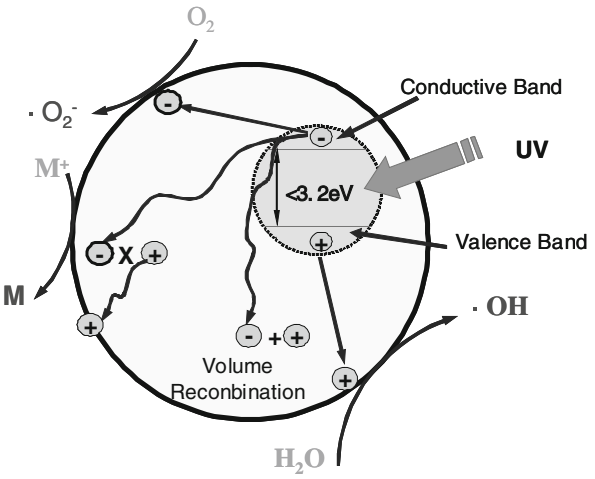

Fig. 11 The principle of photocatalysis

Based upon these postulates, a new simplified mechanism of the TiO_2/OH• action is proposed by the authors:

$$TiO_2 + h\nu \rightarrow TiO_2 + h^+ + e$$

$$H_2O + h^+ \rightarrow OH\bullet + H^+$$

$$OH^- + h^+ \rightarrow OH\bullet$$

$$O_2 + e \rightarrow OH\bullet$$

$$H_2O + O_2^- \rightarrow OOH\bullet + OH^-$$

$$OOH\bullet + H_2O + e \rightarrow H_2O_2 + OH^-$$

For anionic dye-MO

$Ni^{2+} + e \rightarrow Ni$

$MO^- + h^+ \rightarrow$ adsorbed

} complementary function

For cationic dye-Rh.B

$Ni^{2+} + e \rightarrow Ni$

$Rh.B^+ + e \rightarrow$ adsorbed

} competitive function

⇩ More e^- are generated Enhancement

⇩ Less e^- are generated Weakening

⇩

$$H_2O_2 + e \rightarrow OH\bullet + OH^-$$

Conclusion

The degradability of MO and Rh.B by the CTA photocatalyst was examined with or without metal ions being present. Different findings were obtained when CTA dealt with

anionic dye-MO and cationic dye-Rh.B. When the Ni^{2+} load increased from 0 to 31.3 mg/g, the degradation of MO increased by 32.3%, while that of Rh.B decreased by 32.9%. Similar effects were noticed in the presence of Cu^{2+}. Irrespective of the form of the metal ion, the degradation of the MO dye is enhanced and that of Rh.B is inhibited when metal ions are present. With the decreasing pH value, the degradation performance for MO and Rh.B increases, while for Rh.B, this effect is not monotonous and a peak exists. This indicates that protons, as electron acceptor just like metal ions, affect the degradation ability of CTA in a similar way for Ni^{2+} and Cu^{2+}. XPS analyses when Ni^{2+} is present confirms that a lower binding energy of Ni would oppress the recombination rate of e^-/h^+ pairs and result in the improvement of photocatalyses when Ni^{2+} and MO coexisted. The opposite phenomena occur when Ni^{2+} and Rh.B coexist. Since MO and Rh.B possess chromogenic groups with different charges, these groups will differently affect the photo action of TiO_2, leading to a different formation of electron/hole pairs when the process is initiated under UV, thus also affecting the production of OH• which is important during the photocatalysis action of TiO_2.

Acknowledgments The authors want to express their thanks for the support from the Natural Science Foundation of China (20876008, 21076009), the National Basic Research Program (973 Program) of China (2007CB714305), the (863) High Technology Project (2008AA062401), the Chinese Universities Scientific Fund (ZZ1024), and the Program for New Century Excellent Talents in University (NCET-100212).

References

1. Gupta, V. K., Carrott, P. J. M., Ribeiro Carrott, M. M. L., & Suhas (2009). Low cost adsorbents: growing approach to wastewater treatment—a review. *Critical Reviews in Environmental Science and Technology, 39*, 783–842.
2. Van Gauwbergen, D., & Baeyens, J. (2002). Modeling and scale-up of reverse osmosis separation. *Environmental Engineering Science, 19*, 37–45.
3. Baeyens, J., Mochtar, I. Y., Liers, S., & Dewit, H. (1995). Plugflow dissolved air flotation. *Water Environment Research, 67*, 1027–1035.
4. Dewil, R., Appels, L., Baeyens, J., Buczynska, A., & Van Vaeck, L. (2007). The analysis of volatile siloxanes in waste activated sludge. *Talanta, 74*, 14–19.
5. Hall, S., Tang, R., Baeyens, J., & Dewil, R. (2009). Removing polycyclic hydrocarbons from water by adsorption of silica gel. *Polycyclic Aromatic Compounds, 29*, 160–183.
6. Neyens, E., Baeyens, J., Weemaes, M., & De Heyder, B. (2002). Advanced biosolids treatment using H_2O_2-oxidation. *Environmental Engineering Science, 19*, 27–35.
7. Neyens, E., & Baeyens, J. (2003). A review of classic Fenton's peroxidation as an advanced oxidation technique. *Journal of Hazardous Materials, 97*, 295–314.
8. Bailey, S. E., Plin, T. J., Bricka, R. M., & Adrain, D. D. (1999). A review of potentially low cost sorbents for heavy metals. *Water Research, 33*, 2469–2479.
9. Ali, I., & Gupta, V. K. (2006). Advances in water treatment by adsorption technology. *Nature Protocols, 1*, 2661–2667.
10. Gupta, V. K., Mittal, A., Malviya, A., & Mittal, J. (2009). Adsorption of carmoisine A from wastewater using waste materials—bottom ash and deoiled soya. *Journal of Colloid and Interface Science, 335*, 24–33.
11. Gupta, V. K., Mittal, A., Gajbe, V., & Mittal, J. (2008). Adsorption of basic fuchsin using waste materials—bottom ash and deoiled soya as adsorbents. *Journal of Colloid and Interface Science, 319*, 30–39.
12. Gupta, V. K., Mittal, A., Jain, R., Mathur, M., & Sikarwar, S. (2006). Adsorption of Safranin-T from wastewater using waste materials-activated carbon and activated rice husks. *Journal of Colloid and Interface Science, 303*, 80–86.
13. Gupta, V. K., Ali, I., & Saini, V. K. (2007). Adsorption studies on the removal of Vertigo Blue49 and Orange DNA13 from aqueous solutions using carbon slurry developed from a waste material. *Journal of Colloid and Interface Science, 315*, 87–93.

14. Gupta, V. K., Suhas, Ali, I., & Saini, V. K. (2004). Removal of rhodamine B, fast green and methylene blue from wastewater using red mud—an aluminum industry waste. *Industrial and Engineering Chemistry Research, 43*, 1740–1747.
15. Gupta, V. K., Mittal, A., Kurup, L., & Mittal, J. (2006). Adsorption of a hazardous dye, erythrosine, over hen feathers. *Journal of Colloid and Interface Science, 304*, 52–57.
16. Gupta, V. K., Ali, I., Saini, V. K., Gerven, T. V., Bruggen, B. V., & Vandecasteele, C. (2005). Removal of dyes from waste water using bottom ash. *Ind. Engg. Chem. Res., 44*, 3655–3664.
17. Gupta, V. K., Gupta, B., Rastogi, A., Agarwal, S., & Nayak, A. (2011). A comparative investigation on adsorption performances of mesoporous activated carbon prepared from waste rubber tire and activated carbon for a hazardous azo dye-acid blue 113. *J. Hazardous Mat., 186*, 891–901.
18. Gupta, V. K., & Ali, I. (2008). Removal of endosulfan and methoxychlor from water on carbon slurry. *Environmental Science and Technology, 42*, 766–770.
19. Jain, R., Mathur, M., Sikarwar, S., & Mittal, A. (2007). Removal of the hazardous dye rhodamine B through photocatalytic and adsorption treatments. *Journal of Environmental Management, 85*, 956–964.
20. Yu, J. C., Yu, J. G., & Zhao, J. C. (2002). Enhanced photo-catalytic activity of mesoporous and ordinary TiO_2 thin films by sulfuric acid treatment. *Applied Catalysis B: Environmental, 36*, 31–43.
21. Li, J. Y., Chen, C. C., Zhao, J. C., Zhu, H. Y., & Orthman, J. (2002). Photodegradation of dye pollutants on TiO_2 nanoparticles dispersed in silicate under UV–VIS irradiation. *Applied Catalysis B: Environmental, 37*, 331–338.
22. Zertal, A., Molnár-Gábor, D., Malouki, M. A., Sehili, T., & Boule, P. (2004). Photocatalytic transformation of 4-chloro-2-methylphenoxyacetic acid (MCPA) on several kinds of TiO_2. *Applied Catalysis B: Environmental, 49*, 83–89.
23. Han, W. Y., Zhu, W. P., Zhang, P. Y., Zhang, Y., & Li, L. S. (2004). Photocatalytic degradation of phenols in aqueous solution under irradiation of 254 and 185 nm UV light. *Catalysis Today, 90*, 319–324.
24. Wu, C. H., Chang-Chien, G. P., & Lee, W. S. (2004). Photodegradation of polychlorinated dibenzo-p-dioxins: comparison of photocatalysts. *Journal of Hazardous materials B, 114*, 191–197.
25. Jain, R., & Shrivastava, M. (2008). Photocatalytic removal of hazardous dye cyanosine from industrial waste using titanium dioxide. *Journal of Hazardous Materials, 152*, 216–220.
26. Gupta, V. K., Jain, R., Mittal, A., Mathur, M., & Sikarwar, S. (2007). Photochemical degradation of the hazardous dye Safranin-T using TiO2 catalyst. *Journal of Colloid and Interface Science, 309*, 464–469.
27. Parra, S., Sarria, V., Malato, S., Peringer, P., & Pulgarin, C. (2000). Photochemical versus coupled photochemical–biological flow system for the treatment of two biorecalcitrant herbicides: metobromuron and isoproturon. *Applied Catalysis B: Environmental, 27*, 153–168.
28. Macak, J. M., Zlamal, M., Krysa, J., & Schmuki, P. (2007). Self-organized TiO_2 nanotube layers as highly efficient photocatalysts. *Small, 3*, 300–304.
29. Paulose, M., Shankar, K., Varghese, O. K., Mor, G. K., Hardin, B., & Grimes, C. A. (2006). Backside illuminated dye-sensitized solar cells based on titania nanotube array electrodes. *Nanotechnology, 17*, 1446–1448.
30. Tennakone, K., & Wijayantha, K. G. U. (2005). Photocatalysis of CFC degradation by titanium dioxide. *Applied Catalysis B: Environmental, 57*, 9–12.
31. Mozia, S., Tomaszewska, M., & Morawski, A. W. (2005). A new photocatalytic membrane reactor (PMR) for removal of azo-dye Acid Red 18 from water. *Applied Catalysis B: Environmental, 59*, 131–137.
32. Bowering, N., Walker, G. S., & Harrison, P. G. (2006). Photocatalytic decomposition and reduction reactions of nitric oxide over Degussa P25. *Applied Catalysis B: Environmental, 62*, 208–216.
33. Cheung, W. H., Ng, J. C. Y., & McKay, G. (2003). Kinetic analysis of the sorption of copper(II) ions on chitosan. *Journal of Chemical Technology and Biotechnology, 78*, 562–571.
34. Chu, K. H. (2002). Removal of copper from aqueous solution by chitosan in prawn shell: adsorption equilibrium and kinetics. *Journal of Hazardous Materials, 90*, 77–95.
35. Juang, R. S., & Shao, H. J. (2002). A simplified equilibrium model for sorption of heavy metal ions from aqueous solutions on chitosan. *Water Research, 36*, 2999–3008.
36. Chen, S. M., Yen, M. S., & Shen, Y. H. (2010). Effect of chitosan biopolymer and UV/TiO_2 method for the de-coloration of acid blue 40 simulated textile wastewater. *African Journal of Biotechnology, 34*, 5575–5580.
37. Su, H. J., Wang, Z. X., & Tan, T. W. (2005). Preparation of a surface molecular-imprinted adsorbent for Ni^{2+} based on *Penicillium chrysogenum*. *Journal of Chemical Technology and Biotechnology, 80*, 439–444.
38. Zhao, X. L., Li, Q., Zhang, X., Su, H. J., Lan, K., & Chen, A. Z. (2011). Simultaneous removal of metal ions and methyl orange by combined selective adsorption and photocatalysis. *Environmental Progress & Sustainable Energy*. doi:10.1002/ep.10507.

39. Murakami, N., Chiyoya, T., Tsubota, T., & Ohno, T. (2008). Switching redox site of photocatalytic reaction on titanium(IV) oxide particles modified with transition-metal ion controlled by irradiation wavelength. *Applied Catalysis A: General, 348*, 148–152.
40. Teh, C. M., & Mohamed, A. R. (2010). Roles of titanium dioxide and ion-doped titanium dioxide on photocatalytic degradation of organic pollutants (phenolic compounds and dyes) in aqueous solutions: a review. *Journal of Alloys and Compounds, 12*, 117–130.
41. Aarthi, T., & Madras, G. (2008). Photocatalytic reduction of metals in presence of combustion synthesized nano-TiO_2. *Catalysis Communications, 9*, 630–634.
42. Gözmen, B., Turabik, M., & Hesenov, A. (2009). Photocatalytic degradation of Basic Red 46 and Basic Yellow 28 in single and binary mixture by UV/TiO2/periodate system. *Journal of Hazardous Materials, 164*, 1487–1495.
43. Devi, L. G., Murthy, B. N., & Kumar, S. G. (2010). Photocatalytic activity of TiO_2 doped with Zn^{2+} and V^{5+} transition metal ions: influence of crystallite size and dopant electronic configuration on photocatalytic activity. *Materials Science and Engineering B, 166*, 1–6.
44. Huo, H. Y., Su, H. J., Jiang, W., & Tan, T. W. (2009). Effect of trace Ag^{+} adsorption on degradation of organic dye wastes. *Biochemical Engineering Journal, 43*, 2–7.
45. Fu, G. H., Cai, W. P., Gan, Y. J., & Jia, J. H. (2004). Ambience-induced optical absorption peak for Au/SiO_2 mesoporous assembly. *Chemical Physics Letters, 385*, 15–19.
46. Ni, M., Leung, K. H., Leung, Y. C., & Sumathy, K. (2007). A review and recent developments in photocatalytic water-splitting using TiO_2 for hydrogen production. *Renewable and Sustainable Energy Reviews, 11*, 401–425.
47. Abe, R., Sayama, K., & Arakawa, H. (2002). Efficient hydrogen evolution from aqueous mixture of I^{-} and acetonitrile using a merocyanine dye-sensitized Pt=TiO_2 photocatalyst under visible light irradiation. *Chemical Physics Letters, 362*, 441–444.
48. Nie, Y. L., Hu, C., Qu, J. H., & Zhao, X. (2009). Photoassisted degradation of endocrine disruptors over CuO_x–FeOOH with H_2O_2 at neutral pH. *Applied Catalysis B: Environmental, 87*, 30–36.
49. Foster, N. S., Noble, R. D., & Koval, C. A. (1993). Reversible photoreductive deposition and oxidative dissolution of copper ions in titanium dioxide aqueous suspensions. *Environmental Science and Technology, 27*, 350–356.
50. Ward, M. D., & Bard, A. J. (1982). Photocurrent enhancement via trapping of photogenerated electrons of titanium dioxide particles. *Journal of Physical Chemistry, 86*, 3599–3605.
51. Kiwi, J., Pulgarin, C., Peringer, P., & Gratzel, M. (1993). Beneficial effects of homogeneous photo-Fenton pretreatment upon the biodegradation of anthraquinone sulfonate in waste water treatment. *Applied Catalysis B: Environmental, 3*, 85–99.
52. Okamoto, K. I., Yamamoto, Y., Tanaka, H., Tanaka, M., & Itaya, A. (1985). Heterogeneous photocatalytic decomposition of phenol over TiO_2 powder. *Bulletin of the Chemical Society of Japan, 58*, 2015–2022.
53. Okamoto, K. I., Yamamoto, Y., Tanaka, H., & Itaya, A. (1985). Kinetics of heterogeneous photocatalytic decomposition of phenol over anatase TiO_2 powder. *Bulletin of the Chemical Society of Japan, 58*, 2023–2028.
54. Sykora, J. (1997). Photochemistry of copper complexes and their environmental aspects. *Coordination Chemistry Reviews, 159*, 95–108.
55. Butler, E. C., & Davis, A. P. (1993). Photocatalytic oxidation in aqueous titanium dioxide suspensions: the influence of dissolved transition metals. *Journal of Photochemistry and Photobiology A: Chemistry, 70*, 273–283.